Bioelectrochemistry 74 (2008) 157–163

Contents lists available at ScienceDirect

Bioelectrochemistry

journal homepage: www.elsevier.com/locate/bioelechem

Direct electrochemistry and electrochemical catalysis of myoglobin–TiO_2 coated multiwalled carbon nanotubes modified electrode

Lei Zhang [a], Dan-Bi Tian [a,*], Jun-Jie Zhu [b]

[a] College of Science, Nanjing University of Technology, Nanjing 210009, PR China
[b] Key Lab. of Analytical Chemistry for Life Science, Department of Chemistry, Nanjing University, Nanjing 210093, PR China

ARTICLE INFO

Article history:
Received 28 February 2008
Received in revised form 8 July 2008
Accepted 9 July 2008
Available online 17 July 2008

Keywords:
Myoglobin
Multiwalled carbon nanotubes
TiO_2
Electrocatalysis
Electrochemistry

ABSTRACT

TiO_2 nanoparticles were homogeneously coated on multiwalled carbon nanotubes (MWCNTs) by hydrothermal deposition, and this nanocomposite might be a promising material for myoglobin (Mb) immobilization in view of its high biocompatibility and large surface. The glassy carbon (GC) electrode modified with Mb–TiO_2/MWCNTs films exhibited a pair of well-defined, stable and nearly reversible cycle voltammetric peaks. The formal potential of Mb in TiO_2/MWCNTs film was linearly varied in the range of pH 3–10 with a slope of 48.65 mV/pH, indicating that the electron transfer was accompanied by single proton transportation. The electron transfer between Mb and electrode surface, k_s of 3.08 s^{-1}, was greatly facilitated in the TiO_2/MWCNTs film. The electrocatalytic reductions of hydrogen peroxide were also studied, and the apparent Michaelis–Menten constant is calculated to be 83.10 μM, which shows a large catalytic activity of Mb in the TiO_2/MWCNTs film to H_2O_2. The modified GC electrode shows good analytical performance for amperometric determination of hydrogen peroxide. The resultant Mb–TiO_2/MWCNTs modified glassy carbon electrode exhibited fast amperometric response to hydrogen peroxide reduction, long term life and excellent stability. Finally the activity of the sensor for nitric oxide reduction was also investigated.

1. Introduction

There has been increasing interest in studying protein in order to prepare the third generation biosensors. It is difficult for proteins to exchange electrons with electrode surfaces directly, because they usually have large and complex structure, where the redox centers are deeply immersed in the bodies, and three-dimensional structures hinder interaction with the electrode, the adsorptive denaturation of proteins onto electrodes and the unfavorable orientations at the electrode. An approach to realize direct electrochemistry of proteins and enzymes is to incorporate them into films to fabricate a modified electrode surface. Thin films may provide a well-defined microenvironment for proteins, and enhance the direct electron transfer between proteins and electrodes.

Myoglobin (Mb) is a single-chain hemeprotein whose physiological importance is principally related to its ability to bind molecular oxygen. It is found mainly in muscle tissue where it serves as an intracellular storage site for oxygen. Mb contains an iron-containing porphyrin in the center, the electroactive group in Mb is buried within the overall structure, and its interaction with the electrode surface is hindered [1]. To explore the methods of increasing the electron transfer between Mb and the electrode, great efforts have been devoted to the characterization of the electrochemistry of Mb using electrodes modified with films such as surfactants [2–5], polymers [6,7], and distal histidine [8].

Carbon nanotubes (CNTs) have gained considerable attention in recent years for their remarkable electronic and mechanical properties. The closed topology and the tubular structure of CNTs make them unique among different carbon forms and provide useful pathways for chemical studies. The immobilization of proteins on carbon nanotubes has been proved to be an effective method for biosensing applications. Dekker et al. [9] successfully fabricated enzyme-coated carbon nanotubes as a single-molecule sensitive pH biosensor. On the other hand, TiO_2 nanoparticles were used as a film-forming material since they have high surface area, optical transparency, good biocompatibility, and relatively good conductivity. Various TiO_2 films were also used to immobilize proteins or enzymes on electrode surface for either mechanistic study of the proteins or fabricating electrochemical biosensors [10,11]. After being immobilized on nanoscale TiO_2 matrices, the proteins show enhanced electrochemical activity, which allows the electrochemical measurements of their substrates with high sensitivity and improved selectivity [10]. These new hybrid carbon nanotubes with immobilized anatase TiO_2 on the sidewalls may have more interesting biosensor applications that are now under investigation. Taking advantage of the unique electronic properties of the MWCNTs, we expect that the combination of MWCNTs with TiO_2 may induce interesting charge transfer and thus enhance the electrocatalytic activity of enzymatic bioelectrodes.

* Corresponding author.
E-mail address: danbi@njut.edu.cn (D.-B. Tian).

1567-5394/$ – see front matter.
doi:10.1016/j.bioelechem.2008.07.003

Herein, a novel Mb–TiO_2/MWCNTs film biosensor was fabricated to improve their electroactivity for H_2O_2 and NO. The anatase TiO_2 nanoparticles were coupled with MWCNTs successfully via the vapor phase transfer method, and Mb could be immobilized on the surface of TiO_2/MWCNTs film by adsorption. Electrochemical behavior of the sensor was studied in detail. Direct electron transfer between Mb and GC electrode and the electrocatalytic reduction of H_2O_2 and NO at biosensor was observed. This Mb–TiO_2/MWCNT biosensor responded more sensitively to H_2O_2 and NO than those modified by TiO_2 nanoparticles alone.

2. Experimental

2.1. Reagents

MWCNTs with diameters ranging from 20–50 nm and lengths ranging from 0.5 to 500 μm, were provided by Shenzhen Nanotech Port Co. Ltd. Myoglobin (equine heart) was obtained from Sigma and used as received without further purification. The 0.1 mol/L phosphate buffer solution (PBS) of various pHs was prepared by mixing the stock solutions of Na_2HPO_4 and NaH_2PO_4 and adjusted by 0.1 M NaOH and 0.1 M H_3PO_4 solutions. H_2O_2 (30% w/v solution) was purchased from Shanghai Chemical Reagent Company. The concentration of the more diluted hydrogen peroxide solutions prepared was determined by titration with cerium (IV) to a ferroin endpoint. All other chemicals were of analytical grade and used without further purification. All solutions were prepared with redistilled water.

2.2. Synthesis of the TiO_2-coated MWCNTs

The vapor phase transfer (VPT) instrument was used to synthesize TiO_2/MWCNTs, which could reduce the organic template waste by recycling use of the liquid phase consisting of organic template and water [12]. 100 mg of MWCNTs was oxidized in 45 ml of concentrated HNO_3 by refluxing for 6 h in a silicone oil bath at 140 °C. The acid treatment not only shortened MWCNTs but also made the inert tube wall active by grafting –COOH and –OH groups.

Acid-treated MWCNTs (5 mg) and tetrabutyltitanate (100 μL) were added into 4 mL of anhydrous ethanol, after sonicating for 10 min, this solution was transferred into the VPT instrument as a solid phase. The liquid phase at the bottom of the VPT instrument consisted of 4 mL distilled water. Heat treatment on the sealed VPT instrument was conducted at 80 °C for 2.5 h in an oven, and then the solid phase was washed with distilled water three times. The precipitated solid collected by centrifugation, dried at 60 °C in vacuum for 6 h.

2.3. Fabrication of Mb–TiO_2/MWCNTs film modified glassy carbon electrode

Prior to coating, the basal GC electrode (3 mm diameter) was first polished with 0.05 μm alumina slurry, then sonicated in nitric acid (1:1), ethanol and redistilled water in turn. The mixture containing 2 mg/mL Mb and 1 mg/mL TiO_2/MWCNTs was mixed round for 15 min, and then a 10 μL aliquot of the thus-prepared Mb–TiO_2/MWCNTs composite was uniformly cast onto the inverted GC electrode. These as-modified electrodes were dried under ambient conditions.

2.4. Electrochemical measurements

The electrochemical response was measured in a conventional three-electrode system using a modified GC electrode as working electrode, a platinum wire as counter electrode, and a SCE (3.5 M KCl) electrode as reference electrode. All potentials were reported in this context with respect to this reference. Prior to the electrochemical experiments, all PBS was in thoroughly anaerobic conditions by bubbling with high-purity nitrogen. Cyclic voltammetry was carried out in the scan range from 0.2 to −0.8 V. All the experiments were performed at room temperature with a CHI660a workstation (Shanghai Chenhua Co. Ltd., Shanghai, China).

2.5. Spectroscopic analysis and Morphology characterization

The products were characterized by using an X-ray powder diffractometer (XRD, D/max 2550 V) with Cu-Ka radiation. Fourier transform infra (FTIR) spectra were obtained on a NEXUS 670 (Nicolet) FTIR instrument at room temperature. Transmission electron micrographs (TEM) were recorded on a JEOL JEM 200CX transmission electron microscope, using an accelerating voltage of 200 KeV.

3. Results and discussion

3.1. TEM and XRD measurement of TiO_2/MWCNTs

Fig. 1 shows the TEM images of MWCNTs with TiO_2 nanoparticles formed on their outer shell. The size of TiO_2 nanoparticles is in the range of 2–10 nm. The interface between MWCNTs and TiO_2 can clearly be observed, indicating that TiO_2 nanoparticles are well attached on the outermost shell of MWCNTs. XRD patterns of the MWCNTs coated with TiO_2 nanoparticles (a) and the acid-treated MWCNTs (b) are presented in Fig. 2. The peaks from anatase phase of TiO_2 nanoparticles locate at 26° (2θ). The crystal structure of MWCNTs may suffer some damage during the refluxing process in concentrated nitric acid to functionalize and shorten the MWCNTs. It is hard to elicit the characteristic peaks of MWCNTs from the spectrum of TiO_2 coated MWCNTs, that shows the good crystallization of anatase TiO_2 and their fine coating on the MWCNTs. It is shown that anatase TiO_2 nanoparticles have been formed on the surface of MWCNTs. It is also shown that MWCNTs can be used as a support material for anatase TiO_2 for electrochemically beneficial applications.

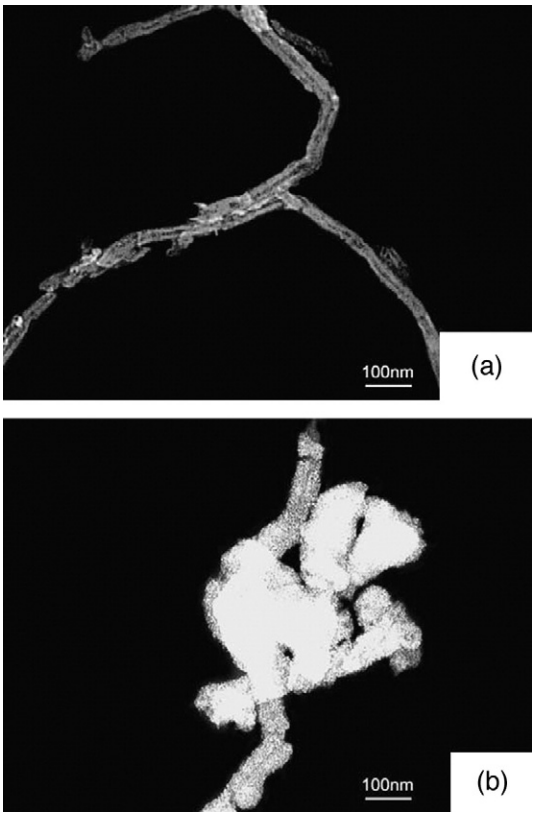

Fig. 1. TEM images of A-MWCNTs (a) and TiO_2/MWCNTs composites (b).

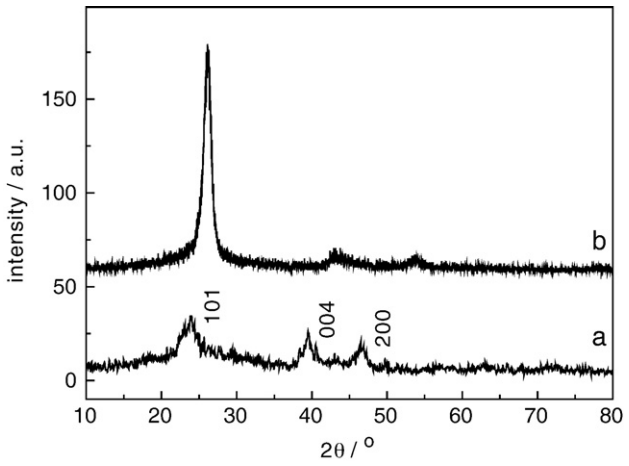

Fig. 2. XRD pattern of TiO_2/MWCNTs (a), acid-treated MWCNTs (b).

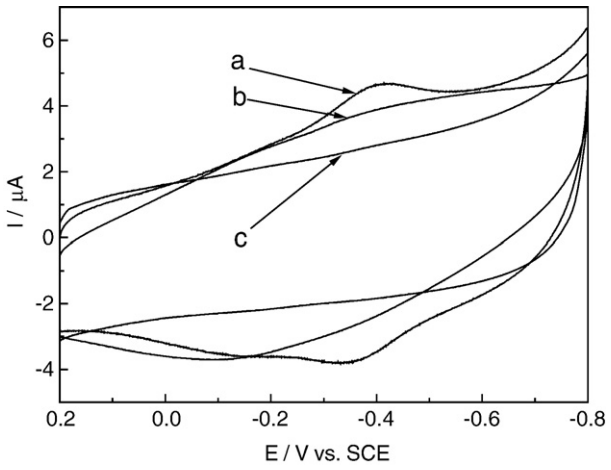

Fig. 4. CVs obtained with Mb–TiO_2/MWCNTs film modified GC electrodes (a), TiO_2/MWCNTs film modified GC electrodes (b) and bare GC electrodes (c) in 0.1 M PBS (pH 7.0) at 100 mV/s.

3.2. FTIR measurement of conformational change

FTIR spectroscopic technique is employed to study the conformational change of Mb on the surface of TiO_2/MWCNTs, since FTIR is very sensitive to the conformational changes of the protein [13–16], and the conformational changes will affect the electron transfer reactivity. It has been known that the shapes of amide I and amide II infrared absorption band of Mb can provide detailed information about the secondary structure of the polypeptide chain [17]. The amide I band (1700–1600 cm^{-1}) is caused by C=O stretching vibrations of peptide linkages in the protein's backbone and the amide II band (1620–1500 cm^{-1}) is attributed to the combination of N–H bending and C–N stretching. In our measurement, the absorption bands of Mb (Fig. 3b) are located at 1654 and 1540 cm^{-1}, which reflect the situation of á helix [18,19] and anti β sheet [20] in the protein, respectively.

Fig. 3a shows the FTIR spectrum of TiO_2/MWCNTs. The oxygen-containing group might be introduced during MWCNTs purification using HNO_3. For MWCNTs coated TiO_2, the absorption bands located at 1037 cm^{-1} are contributed by C–C/C–O stretching vibrations, 1581 cm^{-1} by oxygen-containing groups near C=C, and 1625 cm^{-1} by C=O stretching vibrations as shown in the Fig. 3c. Yates et al. have reported the existence of carboxylic acid and quinone groups on the nanotubes surface after heat treatment by FTIR [21,22]. The peaks of C–C, C=C and oxygen-containing groups also appeared in the FTIR spectrum of Mb–TiO_2/MWCNTs with a slight shift (Fig. 3c). In Fig. 3a, the band about 1641 cm^{-1} in Mb–TiO_2/MWCNTs composite maybe caused by the overlap of the amide I band and the C=O stretching vibration of –COOH (about 1625 cm^{-1}) group in MWCNTs. For amide II, the bands of Mb on the surface of TiO_2/MWCNTs (Fig. 3a) had the similar shapes to that of the free Mb (Fig. 3b), except that the bands had a slight shift (1540 to 1541 cm^{-1}). The above results verified that Mb was adsorbed on the surface of MWCNTs and also indicated that Mb retained its original structure after adsorption [23].

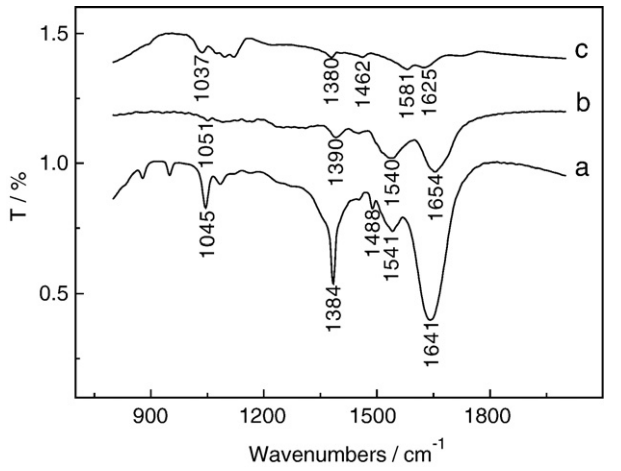

Fig. 3. FTIR spectra of Mb–TiO_2/MWCNTs (a), free Mb (b), TiO_2/MWCNTs (c) film.

3.3. Direct electrochemistry of Mb–TiO_2/MWCNTs film modified electrode

TiO_2/MWCNTs may provide a desirable microenvironment for Mb to undergo facile electron-transfer reactions. Fig. 4 shows the cyclic voltammograms of the Mb–TiO_2/MWCNTs GC electrode (a), TiO_2/MWCNTs GC electrode (b) and bare GC electrode (c). A wide peak (Fig. 4b) is observed, it maybe caused by the redox of the carboxylic acid group of MWCNTs [24,25]. In addition, a pair of well-defined and nearly symmetrical redox peaks is obtained in curve Fig. 4a, this suggest that the redox peaks are ascribed to the electrochemical reaction of Mb immobilized on the surface of TiO_2/MWCNTs. The anodic (E_{pa}) and cathodic (E_{pc}) peak potential are detected at −0.355 V and −0.395 V, respectively, at a scan rate of 100 mV/s. The ratio of anodic to cathodic peak currents is about 0.89, and this indicates that Mb undergoes a quasi-reversible redox process (Fe^{III}/Fe^{II} redox couple)

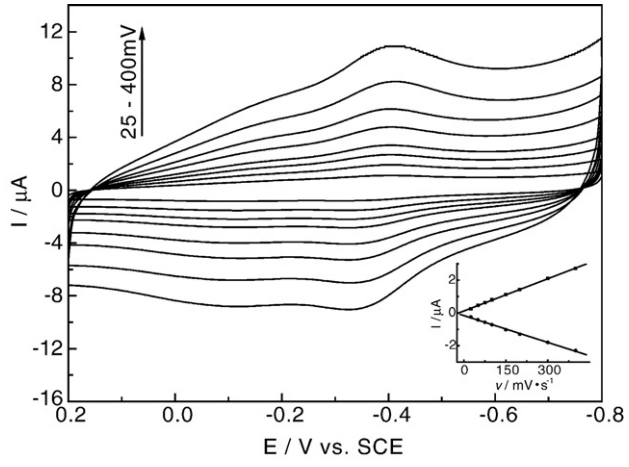

Fig. 5. CVs of Mb–TiO_2/MWCNTs film modified GC electrodes in 0.1 M pH 7.0 PBS at different scan rates. The scan rate from inner to outer are 25, 50, 75, 100, 150, 200, 300, 400 mV/s respectively. Inset: plot of peak currents vs. scan rates.

at the GC electrode modified with TiO_2/MWCNTs film. The separation of peak potentials (ΔE_p) is 40 mV, indicating that Mb immobilized on the surface of TiO_2/MWCNTs display a quasi-reversible electrochemical reaction despite its large molecular structure. Its formal potential ($E^{0\prime}$), which is defined as average of anodic and cathodic peak potentials, was −0.370 V (at 100 mV/s). It was similar to those of other heme-containing proteins (enzymes) including hemoglobin and horseradish peroxidase [26–29].

Fig. 5 shows CVs of Mb–TiO_2/MWCNTs film modified GC electrodes at different scan rate (25–200 mV). With the increase of the scan rate, the redox peak currents (ip) and the peak separation (ΔE_p) increase simultaneously. The peak currents increase linearly in the range from 25 to 200 mV/s, characteristic of a thin layer electrochemical behavior.

$$I_p = \frac{n^2F^2}{4RT} vA\Gamma^* \quad (1)$$

Where A is the effective surface area (7.1×10^{-6} m^2) of the modified electrode, Γ^* is the surface mole density and v is the scan rates, n is the charge transfer number, T=298 K, and the other symbols have their usual meaning. From the integration of the reduction peaks at scan rates less than 200 mV/s, and the surface coverage of Mb on TiO_2/MWCNT GC electrodes is calculated with the following equation to be 8.35×10^{-7} mol/m^2. The value of Γ^* is much greater than theoretical monolayer coverage (counting in one heme-containing chain) of 1.58×10^{-7} mol/m^2 for Mb [27], this value shows the proteins participated in the electron-transfer process in the three-dimensional composite. According to the addition of Mb on GC, the fraction of electroactive Mb is about 7.10% at a rough estimate. This may suggest that only those Mb molecules in the inner layers of the films closest to the electrodes and with a suitable orientation can exchange electrons with the electrode and contribute to the observed redox reaction.

Furthermore, the kinetics of the direct electron transfer is analysed using Laviron model [30]. An estimation of the rate constant (k_s) has been made from the peak potential separation value using the relation given for thin-layer voltammetry [30], a value of 3.08 s^{-1} has been obtained, it also indicates reasonable fast electron transfers between the immobilized Mb molecules and TiO_2/MWCNTs composite.

3.4. Effect of pH

The effect of pH on the potential of the Mb immobilized on TiO_2/MWCNTs film modified GC electrode was studied in different PBS. Cyclic voltammograms of Mb–TiO_2/MWCNTs films show a strong dependence on pH of PBS (Fig. 6). Both reduction and oxidation peak potentials of the Fe^{III}/Fe^{II} redox couple of Mb–TiO_2/MWCNTs GC electrode shift negatively with an increase in pH. The pH dependences of the peak potentials ($E_p=(E_a+E_c)/2$) are expressed as follows: E_p= −48.65·pH+3.61 (R^2=0.9993). This value is a little smaller than that of −57.8 mV/pH at 18 °C for a reversible one-proton-coupled single-electron transfer during electrochemical reduction [31,32], and this may be due to the effect of the protonation states of ligands trans to the heme iron and amino acids around the heme or to the protonation of the water molecules coordinated to the center [32].

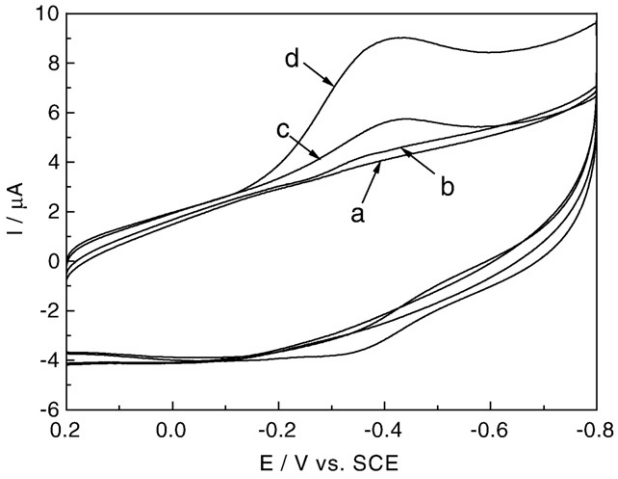

Fig. 7. CVs at 100 mV/s in pH 7.0 PBS for TiO_2/MWCNTs GC electrodes in PBS containing no H_2O_2 (a), as (a) in the presence 0.2 mM of H_2O_2 (b), (c) and (d) as (a) and (b) for Mb–TiO_2/MWCNTs modified GC electrodes.

3.5. Electrocatalysis of Mb–TiO_2/MWCNTs GC electrode to reduction of H_2O_2

It was reported that enzymes and proteins containing heme groups were able to reduce hydrogen peroxide electrocatalytically. In order to verify whether the Mb immobilized on TiO_2/MWCNTs was denatured or not, the electrochemical experiments in the presence of hydrogen peroxide were carried out. Fig. 7 shows cyclic voltammograms of modified electrode in the absence and presence of H_2O_2. As shown in Fig. 7 for bare TiO_2/MWCNTs modified GC electrode, no redox response of H_2O_2 can be seen in the potential range from 0.2 to −0.8 V. However, at the Mb–TiO_2/MWCNTs film modified GC electrode, the reduction current is greatly increased due to catalytic reduction of

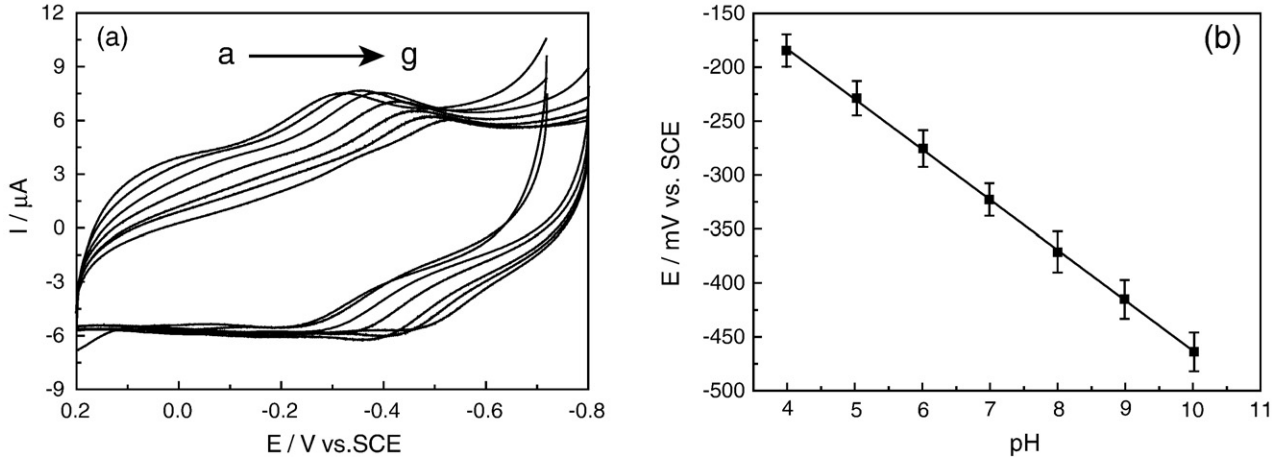

Fig. 6. (A) CVs of Mb–TiO_2/MWCNTs film modified GC electrodes in 0.1 M PBS at various pH values: 5.0 (b), 7.0 (d), 9.0 (f) at scan rate of 100 mV/s. (B) Effect of pH on formal potential of Mb–TiO_2/MWCNTs film modified GC electrodes in 0.1 M PBS.

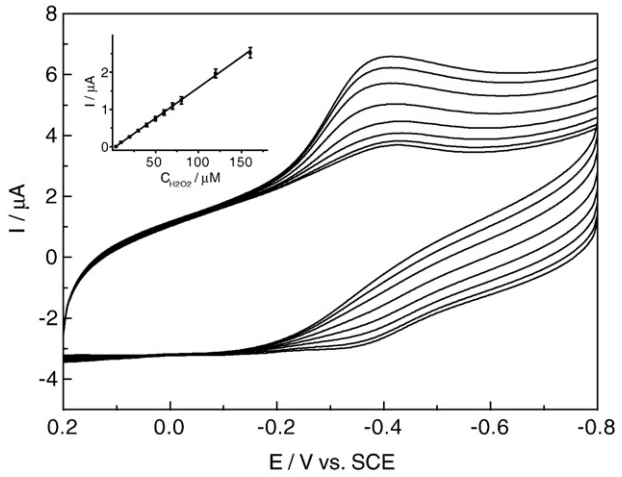

Fig. 8. CVs of Mb–TiO_2/MWCNTs GC electrode in the presence different concentration of H_2O_2 in PBS (pH 7.0) at 100 mV/s, from inner to outer 0, 4, 10, 20, 40, 80, 120 and 160 μM. Inset: the catalytic response vs. hydrogen peroxide concentrations.

hydrogen peroxide, while the oxidation peak has largely disappeared. The decreased overvoltage and increased peak current of hydrogen peroxide reduction confirm that Mb has high catalytic ability for H_2O_2 reduction. Therefore, Mb–TiO_2/MWCNTs composites are suitable for use as mediatorless biosensors.

In order to evaluate the activity of Mb immobilized on TiO_2/MWCNTs film, the cyclic voltammograms of the modified electrode in the presence of different concentrations of hydrogen peroxide were recorded. Fig. 8 shows the cyclic voltammograms for the reduction of hydrogen peroxide on Mb–TiO_2/MWCNTs GC electrode at different concentration range. The catalytic peak currents are proportional to the concentration of H_2O_2 with a linear range from 1 to 160 μM. The linear regression equation for the concentration range from 1–160 μM was $I=0.0164\cdot C-0.0598$, $r=0.9995$. The detection limit is estimated to be 0.41 μM when the signal to noise ratio is 3. At higher hydrogen peroxide concentration, the CV response shows a leveling-off tendency, including a typical Michaelis–Menten process.

The electrocatalytic reduction of hydrogen peroxide at Mb–TiO_2/MWCNTs film modified GC electrode was also studied by hydrodynamic amperometry, which is one of the most widely employed techniques for biosensors. The constant potential of the rotating modified electrode (rotation speed 2000 rpm) was set at −0.4 V after optimization, and the catalytic reduction current was monitored while aliquots of hydrogen peroxide were added. The stepped increase of H_2O_2 concentration in PBS caused the corresponding growth of catalytic reduction currents. As shown in Fig. 9 during the successive addition of 1 μM, 2 μM and 3 μM hydrogen peroxide, a well-defined response is observed (Fig. 9). The plot of response current vs. H_2O_2 concentration is linear over the wide concentration range from 1 to 42 μM. The calibration plot over the concentration range of 1–10 μM has a slope of 17.52 nA/μM (sensitivity), a correlation coefficient of 0.9994 and a detection limit of 0.41 μM, and its response time less than 5 s. When the concentration of hydrogen peroxide is higher than 42 μM, a response plateau was observed, showing the characteristics of the Michaelis–Menten kinetic mechanism. The apparent Michaelis–Menten constant (K_M), which gives an indication of the enzyme–substrate kinetics, can be obtained from the Lineweaver–Burk equation [33]:

$$1/I_{ss} = 1/I_{max} + K_M/I_{max}\cdot 1/C_{H_2O_2}. \quad (2)$$

Here, I_{ss} is the steady-state current after the addition of substrate, C_{H_2O2} is the bulk concentration of substrate and I_{max} is the maximum current measured under saturated substrate solution. K_M can be obtained by the analysis of slope and intercept of the plot of the reciprocals of the steady-state current versus H_2O_2 concentration. The Michaelis–Menten constant of the system (K_M) in this work was found to be 83.10 μM, implying that the Mb–TiO_2/MWCNTs modified GC electrode exhibits a higher affinity for hydrogen peroxide. For comparison, other reported protein films were also listed in Table 1. The Mb–TiO_2/MWCNTs film presents excellent analytical performance in the determination of H_2O_2.

Table 1
Peroxidase-like activity of some protein films

Film	Detection range/μM	Detection limit/μM	K_M/μM
Mb–TiO_2/MWCNTs[a]	1–42	0.41	83
Mb–titanate nanotubes [36]	2–160	0.6	140
Mb–nanocrystalline TiO_2[36]	6–80	3.0	1300
Mb–zirconium phosphonates[37]	–[na]	–[na]	440
Mb–$CaCO_3$ multilayer[38]	5–80	2.0	56
Mb–magadiite nanocomposite[39]	–[na]	–[na]	350

na, not available.
[a] This work.

3.6. Electrocatalysis of Mb–TiO_2/MWCNTs GC electrode toward nitric oxide reduction

Catalytic reduction of NO was studied at the Mb–TiO_2/MWCNTs electrode. As shown in Fig. 10, a new reduction peak appeared at about −0.85 V when NO solution (about 1.6 mM) was added into pH 7.0 PBS,

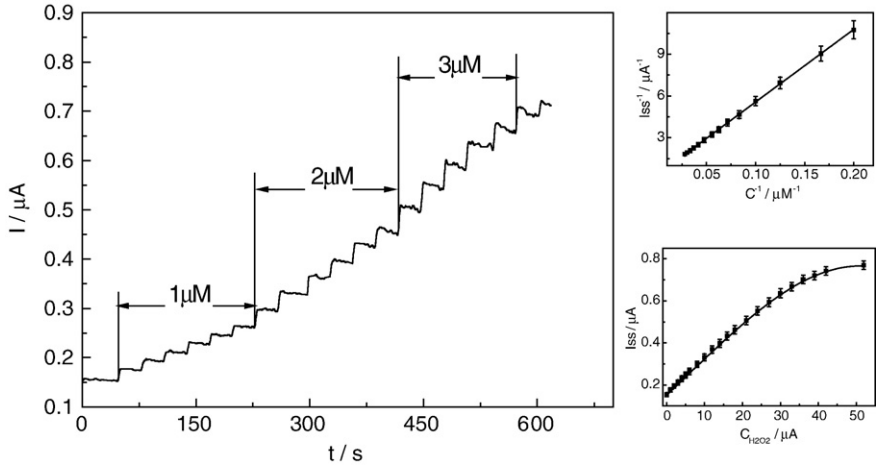

Fig. 9. Amperometric response of Mb–TiO_2/MWCNTs GC electrode with successive addition of H_2O_2 to the 0.1 M pH 7.0 PBS under stirring. The applied potential was −0.4 V.

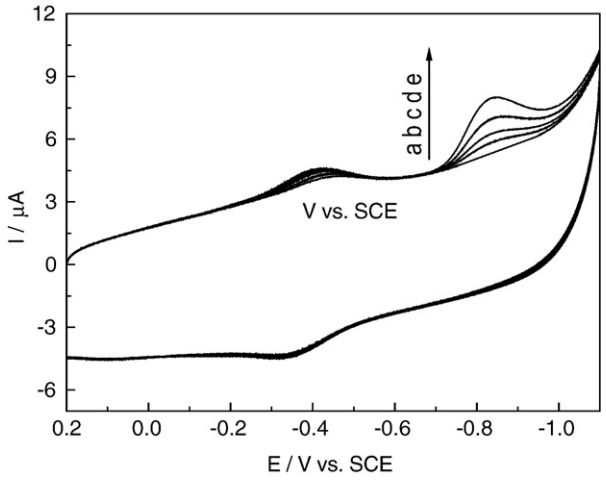

Fig. 10. CVs at 100 mV/s in pH 7.0 PBS for Mb–TiO_2/MWCNTs modified GC electrode in PBS containing no NO (a), as (a) in the presence 0.1, 0.2, 0.4 and 0.8 mM of NO (b, c, d and d).

and the peak current increased with a further addition of NO solution. According to the previous report, this peak correspond to the reduction of NO [35,36], which may be facilitated by electroactive Mb. The possible electrode reaction process can be described as following [34]:

$$Mb(Fe^{II}) + NO \rightarrow Mb(Fe^{II})NO$$

$$2Mb(Fe^{II})NO + 2H^{+} + 2e \rightarrow Mb(Fe^{II}) + N_2O + H_2O$$

Noticeably, no corresponding electrochemical signal is observable either at a bare GC electrode or GC electrode modified with TiO_2 nanoparticles (free of Mb) in the same NO solution until −1.1 V. Therefore the catalytic process comes from the specific enzyme catalytic reaction between Mb and NO, which indicates a large decrease in activation energy for the reduction of NO in the presence of Mb.

3.7. Stability of the biosensor

Long-term stability is one of the most important properties for biosensors and bioreactors. The stability of Mb–TiO_2/MWCNTs films modified electrode was investigated by cyclic voltammetry. The direct electrochemistry of the Mb–TiO_2/MWCNTs modified electrode can retain constant current values upon continuous 200 cyclic sweep over the potential range from −0.8 to 0.2 V at 100 mV/s. After storing it in refrigerator (0 °C) for 30 days, the CV peak potentials remain at the same positions and the reduction peak currents decreased by only about 6.3% of its initial current response. Thus, high stability of modified electrode is related to the chemical stability of TiO_2/MWCNTs film and strong adsorption of Mb on TiO_2/MWCNTs nanoscale islands.

4. Conclusions

A stable Mb–TiO_2/MWCNTs modified electrode was fabricated. Direct electrochemistry of myoglobin was performed at this modified electrode. The modified electrode exhibited a low detection limit of 0.41 μM, a high and reproducible sensitivity of 17.52 nA/μM, a linear range from 1 to 42 μM, and an apparent K_M of 83.10 μM. These parameters demonstrate that TiO_2/MWCNTs provided a favorable microenvironment for direct electron transfer of Mb. The immobilized Mb retained their biological activity and showed a good electrocatalytic response to hydrogen peroxide and nitric oxide reduction. Immobilization of Mb onto TiO_2/MWCNTs film could combine advantages such as high biocompatibility of TiO_2 nanoparticles, large specific surface area for enzyme loading, promoting effect for electron transfer between electrode and Mb, and excellent biocatalytic activity toward hydrogen peroxide and nitric oxide reduction. Finally these nanocomposites were strongly recommended for immobilization of many other enzymes or proteins in fabricating third generation biosensors.

Acknowledgment

We greatly appreciate the support of the National Natural Science Foundation of China (20635020, 90606016).

References

[1] Earle Stellwagen, Haem exposure as the determinate of oxidation–reduction potential of haem proteins, Nature 275 (1978) 73–74.
[2] R. Lin, M. Bayachou, J. Greaves, P.J. Farmer, Nitrite reduction by myoglobin in surfactant films, J. Am. Chem. Soc. 119 (1997) 12689–12690.
[3] N. Hu, J.F. Rusling, Electrochemistry and catalysis with myoglobin in hydrated poly (ester sulfonic acid) ionomer films, Langmuir 13 (1997) 4119–4125.
[4] M. Bayachou, R. Lin, W. Cho, P.J. Farmer, Electrochemical reduction of NO by myoglobin in surfactant film: characterization and reactivity of the nitroxyl (NO−) adduct, J. Am. Chem. Soc. 120 (1998) 9888–9893.
[5] C.E. Immoos, J. Chou, M. Bayachou, E. Blair, J. Greaves, P.J. Farmer, Electrocatalytic reductions of nitrite, nitric oxide, and nitrous oxide by thermophilic cytochrome P450 CYP119 in film-modified electrodes and an analytical comparison of its catalytic activities with myoglobin, J. Am. Chem. Soc. 126 (2004) 4934–4942.
[6] N.Y. Kawahara, W. Ohkubo, H. Ohno, Effect of cast solvent on the electron transfer reaction for poly(ethylene oxide)-modified myoglobin on the electrode in poly (ethylene oxide) oligomers, Bioconjug. Chem. 8 (1997) 244–248.
[7] Y.M. Lvov, Z. Lu, J.B. Schenkman, X. Zu, J.F. Rusling, Direct electrochemistry of myoglobin and cytochrome P450cam in alternate layer-by-layer films with DNA and other polyions, J. Am. Chem. Soc. 120 (1998) 4073–4080.
[8] B.R. Van Dyke, P. Saltman, F.A. Armstrong, Control of myoglobin electron-transfer rates by the distal (nonbound) histidine residue, J. Am. Chem. Soc. 118 (1996) 3490–3492.
[9] K. Besteman, J.O. Lee, F.G.M. Wiertz, H.A. Heering, C. Dekker, Enzyme-coated carbon nanotubes as single-molecule biosensors, Nano Lett. 3 (2003) 727–730.
[10] Y. Zhang, P.L. He, N.F. Hu, Horseradish peroxidase immobilized in TiO_2 nanoparticle films on pyrolytic graphite electrodes: direct electrochemistry and bioelectrocatalysis, Electrochim. Acta 49 (2004) 1981–1988.
[11] A.H. Liu, M.D. Wei, I. Honma, H.S. Zhou, Direct electrochemistry of myoglobin in titanate nanotubes film, Anal. Chem. 77 (2005) 8068–8074.
[12] W. Fan, L. Gao, Silica nanobeads-decorated multi-walled carbon nanotubes by vapor-phase method, Chem. Lett. 34 (2005) 954–955.
[13] H.S., D. Michael Byler, Examination of the secondary structure of proteins by deconvolved FTIR spectra, Biopolymers 25 (1986) 469–487.
[14] W.K. Surewicz, H.H. Mantsch, New insight into protein secondary structure from resolution-enhanced infrared spectra, Biochim. Biophys. Acta 952 (1988) 115–130.
[15] J.K. Koening, D.L. Tabb, Analytical Applications of FTIR to Molecular and Biological Systems, Reidel, Boston MA, 1980, p. 241.
[16] Ronald W. Sarver, William C. Krueger, An infrared and circular dichroism combined approach to the analysis of protein secondary structure, Anal. Biochem. 199 (1991) 61–67.
[17] J.F. Rusling, T.F. Kumosinski, New advances in computer modeling of chemical and biochemical data, Intell. Instrum. Comput. 10 (1992) 139–145.
[18] A. Dong, P. Huang, W.S. Caughey, Protein secondary structures in water from second-derivative amide I infrared spectra, Biochemistry 29 (1990) 3303–3308.
[19] A. Dong, P. Huang, W.S. Caughey, Redox-dependent changes in β-extended chain and turn structures of cytochrome c in water solution determined by second derivative amide I infrared spectra, Biochemistry 31 (1992) 182–189.
[20] S. Krimm, J. Bandekar, Vibrational spectroscopy and conformation of peptides, polypeptides, and proteins, Adv. Protein Chem. 38 (1986) 364.
[21] A. Kuznetsova, D.B. Mawhinney, V. Naumenko, J.T. Yates, J. Liu, R.E. Smalley, Enhancement of adsorption inside of single-walled nanotubes: opening the entry ports, Chem. Phys. Lett. 321 (2000) 292–296.
[22] D.B. Mawhinney, V. Naumenko, A. Kuznetsova, J.T. Yates, J. Liu, R.E. Smalley, Infrared spectral evidence for the etching of carbon nanotubes: ozone oxidation at 298 K, J. Am. Chem. Soc. 122 (2000) 2383–2384.
[23] A.H. Liu, M.D. Wei, I. Honma, H.S. Zhou, Direct electrochemistry of myoglobin in titanate nanotubes film, Anal. Chem. 77 (2005) 8068–8074.
[24] H. Luo, Z. Shi, N. Li, Z. Gu, Q. Zhuang, Investigation of the electrochemical and electrocatalytic behavior of single-wall carbon nanotube film on a glassy carbon electrode, Anal. Chem. 73 (2001) 915–920.
[25] H.X. Luo, Z.J. Shi, N.Q. Li, Z.N. Gu, Q.K. Zhuang, Investigation on the electrochemical and electrocatalytic behavior of chemically modified electrode of single wall carbon nanotube functionalized with carboxylic acid group, Chem. J. Chin. Univ. 21 (2000) 1372–1374.
[26] Q. Lu, T. Zhou, S.S. Hu, Direct electrochemistry of hemoglobin in PHEA and its catalysis to H_2O_2, Biosens. Bioelectron. 22 (2007) 899–904.
[27] H.H. Liu, Z.Q. Tian, Z.X. Lu, Z.L. Zhang, M. Zhang, D.W. Pang, Direct electrochemistry and electrocatalysis of heme-proteins entrapped in agarose hydrogel films, Biosens. Bioelectron. 20 (2004) 294–304.
[28] H.H. Liu, H.Q. Wan, G.L. Zou, Direct electrochemistry and electrochemical catalysis of immobilized hemoglobin in an ethanol–water mixture, Anal. Bioanal. Chem. 385 (2006) 1470–1476.

[29] Q. Xu, C. Mao, N.N. Liu, J.J. Zhu, J. Sheng, Direct electrochemistry of horseradish peroxidase based on biocompatible carboxymethyl chitosan–gold nanoparticle nanocomposite, Biosens. Bioelectron. 22 (2006) 768–773.
[30] E. Laviron, General expression of the linear potential sweep voltammogram in the case of diffusionless electrochemical systems, J. Electroanal. Chem. 101 (1979) 19–28.
[31] A.E.F. Nassar, Z. Zhang, N. Hu, J.F. Rusling, T.F. Kumosinski, Proton-coupled electron transfer from electrodes to myoglobin in ordered biomembrane-like films, J. Phys. Chem. B 101 (1997) 2224–2231.
[32] H. Huang, P. He, N. Hu, Y. Zeng, Electrochemical and electrocatalytic properties of myoglobin and hemoglobin incorporated in carboxymethyl cellulose films, Bioelectrochemistry 61 (2003) 29–38.
[33] R.A. Kamin, G.S. Wilson, Rotating ring-disk enzyme electrode for biocatalysis kinetic studies and characterization of the immobilized enzyme layer, Anal. Chem. 52 (1980) 1198–1205.
[34] L.B. Shang, X.J. Liu, J. Zhong, C.H. Fan, I. Suzuki, G.X. Li, Fabrication of ultrathin, protein-containing films by layer-by-layer assembly and electrochemical characterization of hemoglobin entrapped in the film, Chem. Lett. 32 (2003) 296.
[35] C.H. Fan, G.X. Li, J.Q. Zhu, D.X. Zhu, A reagentless nitric oxide biosensor based on hemoglobin–DNA films, Anal. Chim. Acta 423 (2000) 95–100.
[36] C.H. Fan, J.T. Pang, P.P. Shen, G.X. Li, D.X. Zhu, Nitric oxide biosensors based on Hb/phosphatidylcholinefilms, Anal. Sci. 18 (2002) 129–132.